

Supporting information for

Selection of promising novel fragment sized *S. Aureus* SrtA noncovalent inhibitors based on QSAR and docking modeling studies

Dmitry A. Shulga^{1,*}, Konstantin V. Kudryavtsev^{2,3,*}

¹Department of Chemistry, Lomonosov Moscow State University, Leninskie Gory 1/3, 119991, Moscow, Russian Federation;

²Laboratory of Molecular Pharmacology, Pirogov Russian National Research Medical University, Ostrovityanova Street 1, 117997, Moscow, Russian Federation,

³Laboratory of Chemical Synthesis and Catalysis, Moscow Institute of Physics and Technology, Institutskiy per. 9, 141701, Dolgoprudny, Moscow Region, Russian Federation

*Correspondence: dmitry.a.shulga@gmail.com; konstantin@kudryavtsev.ru; Tel.: +79037640655

Tables S1-S4 and S11 are provided as separate tab-separated-value (TSV) file amenable for both Excel and machine learning analysis.

Table S1-S4 and S9 titles.

Table S1. A set of active compounds used for QSAR classification model building.

Table S2. A set of inactive compounds used for QSAR classification model building.

Table S3. A set of active compounds used for QSAR regression model building. The IC50 activity values (“Act” column) are in nM.

Table S4. A set of inactive compounds used for QSAR regression model building. The IC50 activity values (“Act” column) are in nM.

Table S11. A set of prospective ligands with calculated descriptor values.

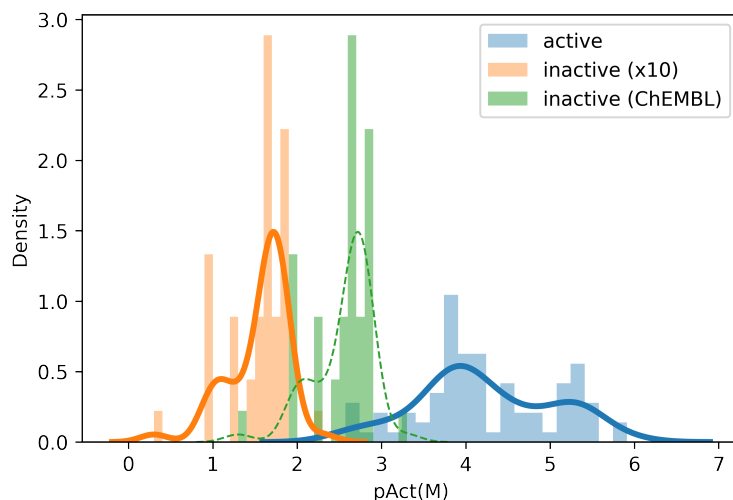


Figure S1. Distribution of activity of structures for regression model building. Activity is in - $\log_{10}(\text{Act}, \text{M})$. The array threshold values are provided in “inactive (ChEMBL)” set, whereas the adjusted data used in modeling are designated as “inactive (x10)”.

Scan for the L1-regularization parameters

1. Classification models

1.1 Support vector machine (SVM)

The models were built using `sklearn.svm.LinearSVC`

(<https://scikit-learn.org/stable/modules/generated/sklearn.svm.LinearSVC.html>), with `penalty='l1'` and `dual=False` settings. The regularization parameter C was varied. The strength of the regularization is inversely proportional to C.

Accuracy is the ratio of correctly predicted actives and inactives to the number of data points,
accuracy = $\text{TP} + \text{TN} / (\text{TP} + \text{TN} + \text{FP} + \text{FN})$.

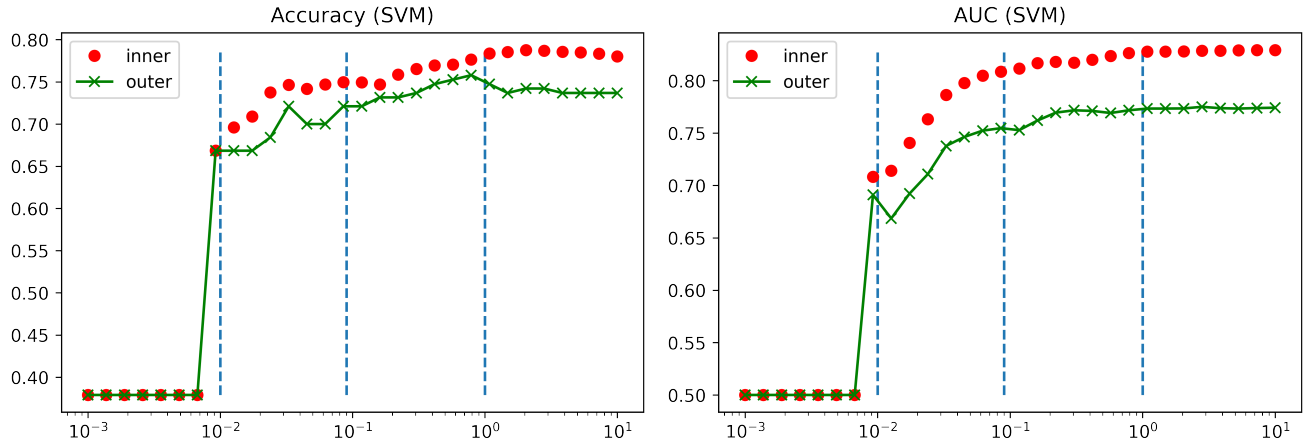


Figure S2. Dependence of the accuracy and the area under curve (AUC) on the regularization parameter C. The metrics are estimated on either the ‘inner’ (the training) set or the ‘outer’ (Leave-one-out) test. The vertical lines correspond to the three parameters used to produce three different models in the manuscript, corresponding to $C=1e-2$, $9e-2$, 1 .

1.2 Logistic regression (LR) classification

The model was built using `sklearn.linear_model.LogisticRegression` with `penalty="l1"` and `solver="liblinear"`

(https://scikit-learn.org/stable/modules/generated/sklearn.linear_model.LogisticRegression.html). The regularization parameter C was varied. The strength of the regularization is inversely proportional to C.

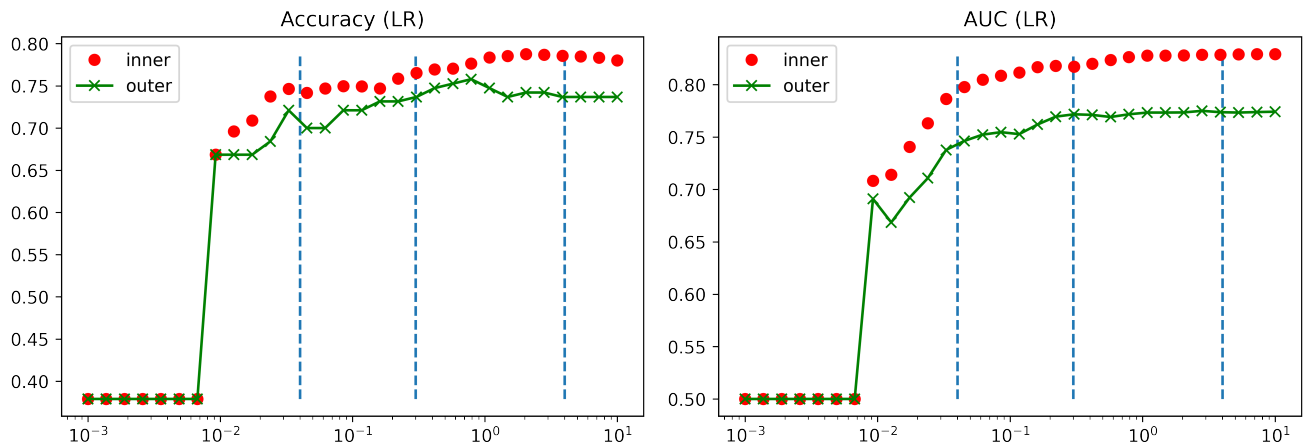


Figure S3. Dependence of the accuracy and the area under curve (AUC) on the regularization parameter C. The metrics are estimated on either the ‘inner’ (the training) set or the ‘outer’ (Leave-one-out) test. The vertical lines correspond to the three parameters used to produce three different models in the manuscript, corresponding to $C=4e-2$, $3e-1$, 4 .

2. Regression models

2.1 LASSO regression

The model was built using `sklearn.linear_model.Lasso` (https://scikit-learn.org/stable/modules/generated/sklearn.linear_model.Lasso.html). The regularization parameter alpha was varied. Larger values of alpha correspond to stronger regularization.

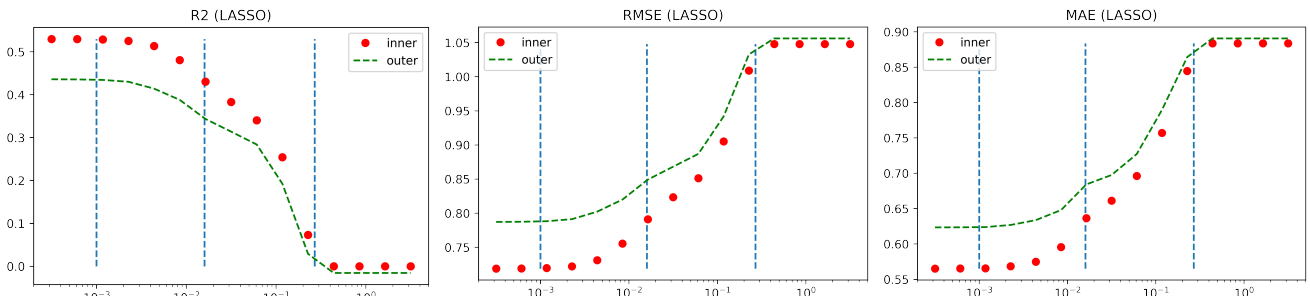


Figure S4. Dependence of R^2 , RMSE and MAE on the value of regularization parameter alpha. The metrics are estimated on either the ‘inner’ (the training) set or the ‘outer’ (Leave-one-out) test. The vertical lines correspond to the three parameters used to produce three different models in the manuscript, corresponding to alpha=1e-3, 1.6e-2, 2.7e-1.

2.2 Support vector machine regression (SVR)

The model was built using `sklearn.svm.SVR` (<https://scikit-learn.org/stable/modules/generated/sklearn.svm.SVR.html>) using kernel="rbf". The regularization parameter C was varied (scaling L2-norm). The strength of the regularization is inversely proportional to C.

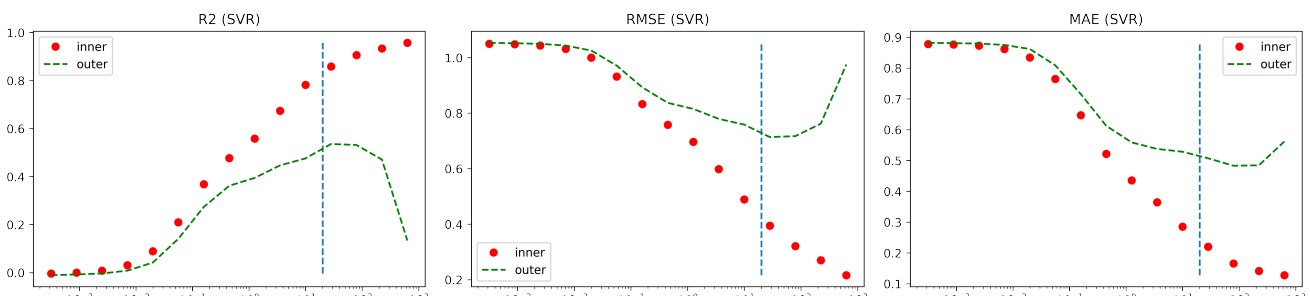


Figure S5. Dependence of R^2 , RMSE and MAE on the value of regularization parameter alpha. The metrics are estimated on either the ‘inner’ (the training) set or the ‘outer’ (Leave-one-out) test. The vertical line correspond to the parameter value used to produce the model in the manuscript, corresponding to C=20.

Table S5. Correlation of the descriptors with activity for classification model molecule set and final decision on using descriptors in model building.

| # | Descriptor | Mean value (std. dev.), unscaled | Correlation | Use in models |
|----|---------------------|----------------------------------|-------------|---------------|
| 1 | MolLogP | 3.3 (1.8) | -0.36 | yes |
| 2 | TPSA | 71.7 (32.7) | 0.10 | no |
| 3 | NHOHCount | 1.8 (1.5) | -0.093 | no |
| 4 | NOCount | 5.0 (2.0) | 0.13 | no |
| 5 | NumHAcceptors | 4.3 (1.9) | 0.18 | yes |
| 6 | NumHDonors | 1.8 (1.3) | -0.12 | yes |
| 7 | NumRotatableBonds | 5.4 (3.9) | -0.032 | yes |
| 8 | NumHeteroatoms | 5.7 (2.5) | 0.16 | yes |
| 9 | FractionCSP3 | 0.3 (0.2) | -0.065 | yes |
| 10 | BalabanJ | 2.5 (0.5) | 0.0003 | no |
| 11 | Chi0 | 35.2 (14.8) | -0.18 | no |
| 12 | Chi1 | 20.1 (7.7) | -0.18 | no |
| 13 | Chi3v | 3.6 (1.4) | -0.085 | no |
| 14 | Chi4v | 2.5 (1.2) | -0.071 | no |
| 15 | HallKierAlpha | -2.2 (0.7) | -0.10 | no |
| 16 | Kappa1 | 5.2 (1.8) | 0.018 | no |
| 17 | Kappa2 | 6.5 (2.7) | -0.058 | no |
| 18 | Kappa3 | 3.2 (1.7) | 0.022 | no |
| 19 | BertzCT | 1690.3 (703) | -0.20 | no |
| 20 | NumAliphaticRings | 1.6 (1.8) | -0.0032 | yes |
| 21 | NumAromaticRings | 2.0 (1.1) | -0.14 | yes |
| 22 | NumAtoms | 45.0 (18.0) | -0.18 | no |
| 23 | MolWt | 357.2 (116.8) | -0.13 | no |
| 24 | MolMR | 96.0 (30.0) | -0.17 | no |
| 25 | MaxPartialCharge | 0.3 (0.1) | -0.097 | yes |
| 26 | MinPartialCharge | -0.4 (0.1) | 0.22 | yes |
| 27 | MaxAbsPartialCharge | 0.4 (0.1) | -0.25 | yes |
| 28 | NumChiralCenters | 1.3 (2.2) | -0.17 | yes |

Table S6. Conformance of mean descriptor values to drug-like and lead-like filters.

| # | Descriptor | Mean (std.dev.) value on the set | Ro5 threshold | Ghose threshold | Veber threshold | Ro3 threshold |
|---|-------------------|----------------------------------|---------------|---------------------|-----------------|---------------|
| 1 | MolLogP | 3.3 (1.8) | 5 | within -0.4 .. +5.6 | | <=3 |
| 2 | MolWt | 357 (117) | 500 | within 180 .. 480 | | <300 |
| 3 | NumHDonors | 1.8 (1.3) | <=5 | | | <=3 |
| 4 | NumHAcceptors | 4.3 (1.9) | <=10 | | | <=3 |
| 5 | NumRotatableBonds | 5.4 (3.9) | | | <=10 | <=3 |
| 6 | MolMR | 96 (30) | | within 40 .. 130 | | |
| 7 | NumAtoms | 45 (18) | | within 20 .. 70 | | |

Table S7. Coefficient values for the production SVM and LR models (9 descriptors).

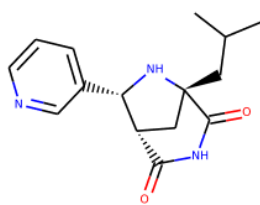
| # | Descriptors | SVM value (lower; upper bounds) ^a | LR value (lower; upper bounds) ^a |
|----|---------------------|--|---|
| 1 | MolLogP | -0.25 (-0.41; -0.06) | -0.61 (-1.09; -0.16) |
| 2 | NumHAcceptors | 0.08 (0.00; 0.29) | 0.22 (0.00; 0.76) |
| 3 | NumHDonors | -0.09 (-0.25; 0.00) | -0.20 (-0.62; 0.00) |
| 4 | NumRotatableBonds | 0.02 (-0.06; 0.21) | 0.03 (-0.14; 0.49) |
| 5 | NumHeteroatoms | 0.14 (0.00; 0.39) | 0.32 (0.00; 0.94) |
| 6 | FractionCSP3 | 0.00 | 0.00 |
| 7 | NumAliphaticRings | 0.00 | 0.00 |
| 8 | NumAromaticRings | -0.06 (-0.28; 0.00) | -0.07 (-0.65; 0.00) |
| 9 | MaxPartialCharge | -0.09 (-0.25; 0.00) | -0.19 (-0.59; 0.00) |
| 10 | MinPartialCharge | 0.00 | 0.00 |
| 11 | MaxAbsPartialCharge | -0.12 (-0.28; 0.00) | -0.31 (-0.68; 0.00) |
| 12 | NumChiralCenters | -0.11 (-0.33; 0.00) | -0.19 (-0.77; 0.00) |

^a Confidence intervals at 95% level obtained using the bootstrap method.

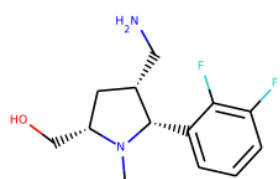
Table S8. Predictions made by classification SVM and LR models for the prospective molecule list.

| # | Structure | SVM, activity | SVM, activity rank* | SVM, predicted value | LR, activity | LR, activity rank* | LR, predicted value |
|----|-----------|---------------|---------------------|----------------------|--------------|--------------------|---------------------|
| 1 | KUD1008 | 0 | 18 | -0.03 | 1 | 17 | 0.19 |
| 2 | KUD1022 | 0 | 19 | -0.05 | 0 | 20 | -0.13 |
| 3 | KUD1036 | 1 | 16 | 0.14 | 1 | 15 | 0.35 |
| 4 | KUD1044 | 1 | 8 | 0.25 | 1 | 8 | 0.61 |
| 5 | KUD1050 | 0 | 24 | -0.50 | 0 | 24 | -1.08 |
| 6 | KUD1066 | 1 | 6 | 0.30 | 1 | 6 | 0.69 |
| 7 | KUD1130 | 1 | 5 | 0.36 | 1 | 7 | 0.68 |
| 8 | KUD1132 | 1 | 14 | 0.21 | 1 | 13 | 0.50 |
| 9 | KUD1133 | 0 | 22 | -0.12 | 0 | 22 | -0.31 |
| 10 | KUD1134 | 1 | 12 | 0.23 | 1 | 14 | 0.47 |
| 11 | KUD1135 | 0 | 20 | -0.07 | 0 | 21 | -0.18 |
| 12 | KUD138 | 1 | 2 | 0.52 | 1 | 2 | 1.21 |
| 13 | KUD165 | 1 | 9 | 0.24 | 1 | 10 | 0.54 |
| 14 | KUD224 | 1 | 11 | 0.23 | 1 | 12 | 0.53 |
| 15 | KUD225 | 1 | 10 | 0.24 | 1 | 11 | 0.54 |
| 16 | KUD233 | 1 | 17 | 0.06 | 1 | 18 | 0.18 |
| 17 | KUD529 | 1 | 15 | 0.15 | 1 | 16 | 0.33 |
| 18 | KUD530 | 1 | 13 | 0.23 | 1 | 9 | 0.56 |
| 19 | KUD649 | 1 | 3 | 0.44 | 1 | 4 | 1.07 |
| 20 | KUD718 | 1 | 1 | 0.69 | 1 | 1 | 1.68 |
| 21 | KUD759 | 0 | 23 | -0.16 | 0 | 23 | -0.33 |
| 22 | KUD833 | 1 | 4 | 0.43 | 1 | 3 | 1.17 |
| 23 | KUD834 | 1 | 7 | 0.27 | 1 | 5 | 0.75 |
| 24 | KUD990 | 0 | 21 | -0.08 | 0 | 19 | -0.06 |

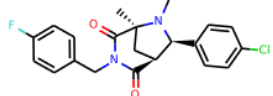
* 1 – the most active structure, 24 – the least active structure according to prediction.



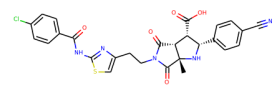
KUD718



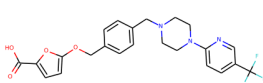
KUD138



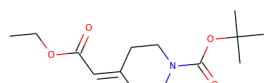
KUD649



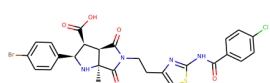
KUD833



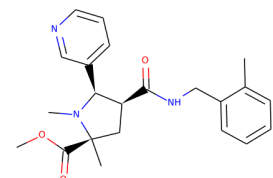
KUD1066



KUD1130

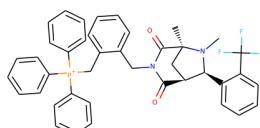


KUD834

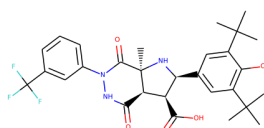


KUD1044

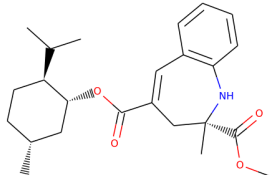
Figure S6. The most active predicted by SVM and LR models molecules. Each structure is represented with a random enantiomer, indistinguishable by the classification models used.



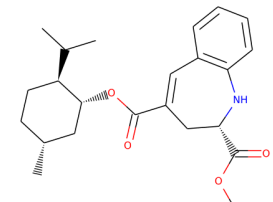
KUD1050



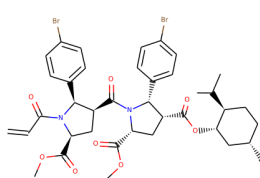
KUD759



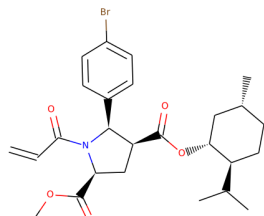
KUD1133



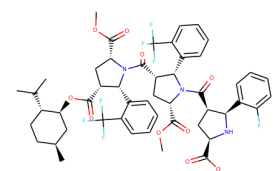
KUD1135



KUD990



KUD1022



KUD1008*

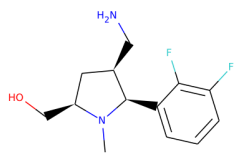
Figure S7. The most probably inactive molecules predicted by SVM and LR models. Each structure is represented with a random enantiomer, indistinguishable by the classification models used.

*KUD1008 was predicted active according to LR model.

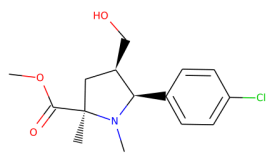
Table S9. Predictions made by regression LASSO and SVR models for the prospective molecule list.

| # | Structure | Lasso, log (Atc., M) | Lasso, LE | SVR, log (Act., M) | SVR, LE |
|----|-----------|----------------------|-----------|--------------------|---------|
| 1 | KUD1008 | 0.6 | -0.01 | -3.4 | 0.07 |
| 2 | KUD1022 | -1.8 | 0.07 | -2.6 | 0.11 |
| 3 | KUD1036 | -2.6 | 0.11 | -3.2 | 0.14 |
| 4 | KUD1044 | -2.7 | 0.13 | -2.7 | 0.13 |
| 5 | KUD1050 | -2.0 | 0.06 | -3.2 | 0.09 |
| 6 | KUD1066 | -3.4 | 0.14 | -3.2 | 0.13 |
| 7 | KUD1130 | -4.1 | 0.30 | -3.6 | 0.26 |
| 8 | KUD1132 | -3.0 | 0.17 | -4.5 | 0.26 |
| 9 | KUD1133 | -2.9 | 0.14 | -3.1 | 0.15 |
| 10 | KUD1134 | -3.7 | 0.22 | -4.2 | 0.25 |
| 11 | KUD1135 | -3.0 | 0.15 | -3.3 | 0.16 |
| 12 | KUD138 | -3.3 | 0.26 | -4.6 | 0.36 |
| 13 | KUD165 | -3.0 | 0.21 | -3.9 | 0.27 |
| 14 | KUD224 | -3.2 | 0.22 | -3.6 | 0.25 |
| 15 | KUD225 | -3.0 | 0.21 | -3.8 | 0.26 |
| 16 | KUD233 | -2.9 | 0.18 | -3.3 | 0.20 |
| 17 | KUD529 | -2.5 | 0.10 | -3.4 | 0.14 |
| 18 | KUD530 | -2.7 | 0.13 | -3.6 | 0.17 |
| 19 | KUD649 | -2.6 | 0.13 | -3.9 | 0.20 |
| 20 | KUD718 | -3.5 | 0.24 | -3.6 | 0.25 |
| 21 | KUD759 | -2.7 | 0.09 | -3.3 | 0.11 |
| 22 | KUD833 | -2.7 | 0.10 | -3.0 | 0.11 |
| 23 | KUD834 | -2.3 | 0.08 | -3.0 | 0.11 |
| 24 | KUD990 | -0.2 | 0.01 | -3.4 | 0.09 |

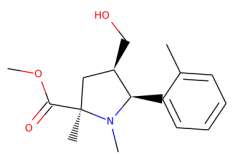
* For activity coloring $\log(\text{Act., M})$ value of -3.0 is taken for white; for LE coloring 50% percentile for both column values is taken for white. $\text{LE} = -0.6 \cdot \ln(10) \cdot \log(\text{Act., M}) / \text{NH}$ [$\text{kcal} \cdot \text{mol}^{-1} \cdot \text{atom}^{-1}$], where NH – is the number of heavy atoms. That conforms to the generally accepted definition of $\text{LE} = -\Delta G / \text{NH} = -RT \cdot \ln(\text{Act}) / \text{NH}$.



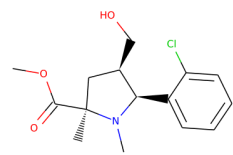
KUD138



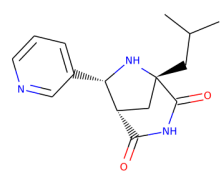
KUD165



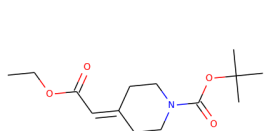
KUD224



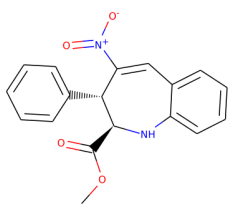
KUD225



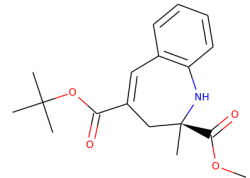
KUD718



KUD1130

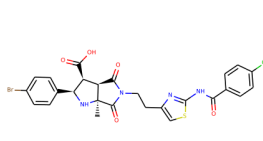


KUD1132

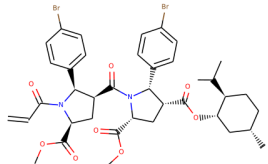


KUD1134

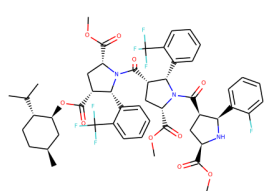
Figure S8. The most active and most efficient (high LE) molecules according to consensus LASSO and SVR models predictions. Each structure is represented with a random enantiomer, indistinguishable by the regression models used.



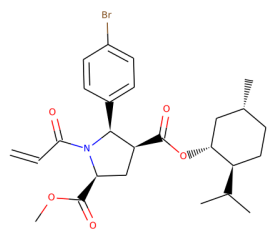
KUD834



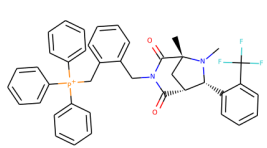
KUD990



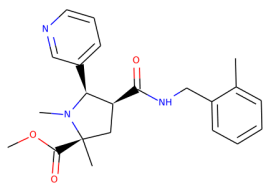
KUD1008



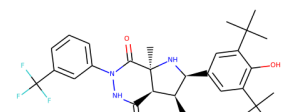
KUD1022



KUD1050



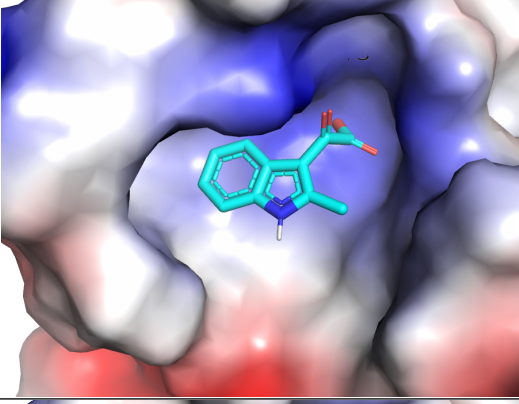
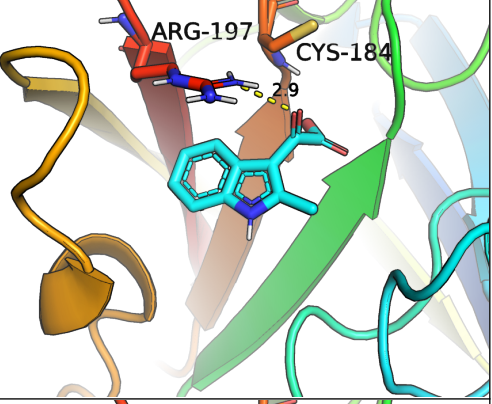
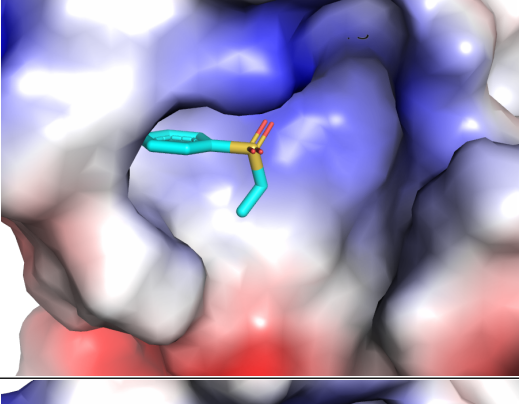
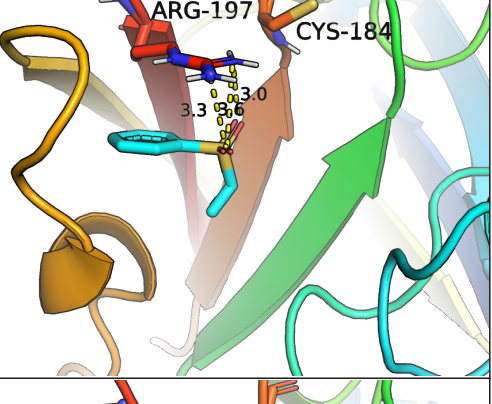
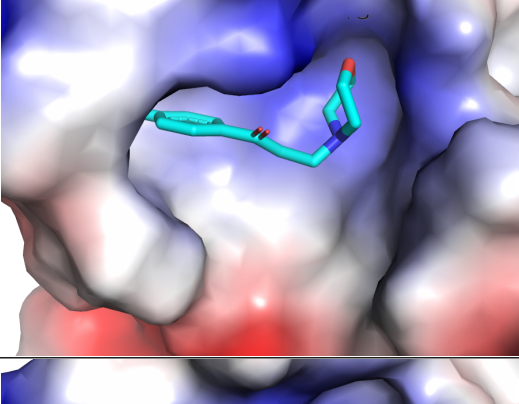
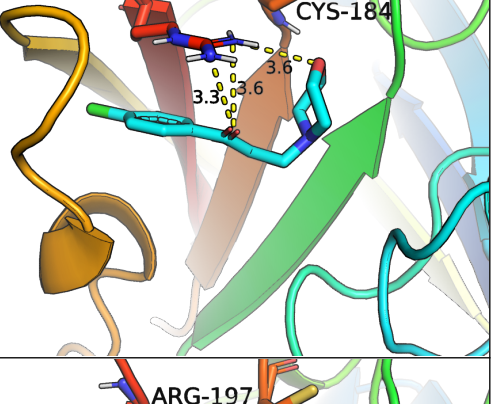
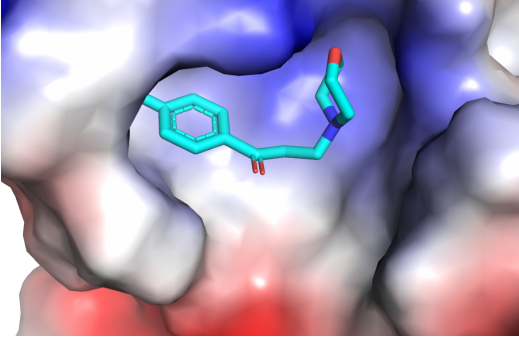
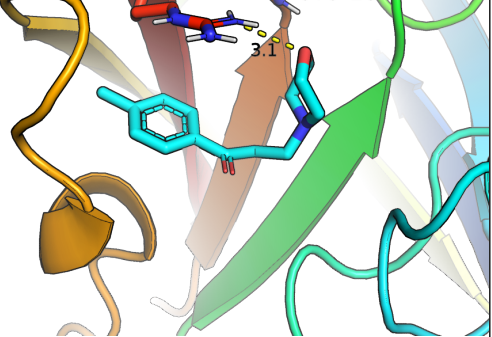
KUD1044*



KUD759**

Figure S9. The least active and least efficient (low LE) molecules according to consensus LASSO and SVR models predictions. Each structure is represented with a random enantiomer, indistinguishable by the classification models used. * present in the least active molecules. ** present in the least efficient molecules.

Table S10. The favorable binding modes according to AutoDock Vina docking for Ro3 subset of active ChEMBL molecules. SrtA model – PDB:2KID. Potential hydrogen bond (electrostatic) interactions of the ligands with Arg197 are highlighted, the distances are between heavy atoms in Å.

| Num | ChEMBL id | Surface | Bonds |
|-----|---------------|---|--|
| 1 | CHEMBL1288785 |  |  |
| 2 | CHEMBL165058 |  |  |
| 3 | CHEMBL234180 |  |  |
| 4 | CHEMBL258985 |  |  |

